Anal Bioanal Chem (2004) 379 : 640–645
DOI 10.1007/s00216-004-2528-y

SPECIAL ISSUE PAPER

**Markus Nuspl · Wolfhard Wegscheider · Johann Angeli
Wilhelm Posch · Michael Mayr**

Qualitative and quantitative determination of micro-inclusions by automated SEM/EDX analysis

Received: 2 December 2003 / Revised: 14 January 2004 / Accepted: 28 January 2004 / Published online: 18 February 2004
© Springer-Verlag 2004

Abstract With the help of an automated SEM/EDX analysis system non-metallic micro-inclusions in steel can be detected on a metallographically prepared surface area. The system makes it possible to determine position, size, shape and composition of each particle. Usually more than 1000 inclusions are found on one scan area. Therefore a new offline evaluation method has been developed to classify the large amount of inclusions and calculate specific size and shape data. A summary sheet is created to show the area contents and the mean values of all important properties for each class. Size and *XY* distributions as well as binary and ternary phase diagrams are drawn to depict the results. The strengths of this analytical technique are demonstrated by evaluation of an LC (low-carbon) steel. Alumina, common spinel, sulfide and oxisulfide inclusions could be identified as dominant inclusion types in LC steel.

Keywords Automated SEM/EDX analysis · Non-metallic inclusion · Micro-inclusion · LC steel

Introduction

Steel cleanliness is determined by number, size, shape and composition of non-metallic inclusions. Because of their detrimental and often decisive effect on material properties, exact determination of non-metallic inclusions is essential. These negative effects are strongly dependent on the application of the produced steel grade. Especially oxide inclusions can result in poor fatigue characteristics of the material. During rolling dendrites and aggregates fracture mainly along necks and subgrains. This results in elongated strings of fragmented particles which at high strains may initiate fatigue. The critical size of a potentially detrimental oxide inclusion at the surface is 8 to 10 μm [1].

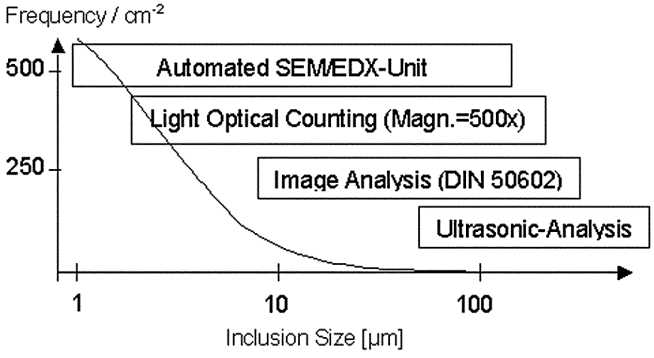

Fig. 1 Size range of cleanliness assessing methods and usual size distribution of inclusions

Nowadays inclusions are subdivided into macro- (>20 μm), micro- (1–20 μm) and submicro-inclusions (<1 μm) [2] and it is in general impossible to analyse inclusions of all size classes simultaneously. Therefore many methods for inclusion analysis are in use and each one can determine particles of a certain size range. Figure 1 lists generally employed techniques along with the automated SEM/EDX system used for cleanliness measurements at **voest**alpine. The size ranges of their application are shown by the widths of the boxes and the curve gives a typical inclusion size distribution.

Figure 1 pinpoints two of the most important advantages of the automated SEM/EDX unit. Both the range of size detection capability and the number of inclusions detectable are large. The latter is illustrated by the rise of the size distribution function towards small sizes.

Such SEM/EDX analysis produces a large quantity of raw data that requires special efforts in compiling and condensing these data in tabular form [3]. For this purpose an offline evaluation programme has been developed.

In the following text the experimental principle of automated SEM/EDX analysis and typical results from eval-

M. Nuspl (✉) · J. Angeli · W. Posch · M. Mayr
voestalpine Stahl GmbH,
Voest-Alpine-Str. 3, P.O. Box 3, 4031 Linz, Austria
e-mail: markus.nuspl@voestalpine.com

W. Wegscheider
Institute for General and Analytical Chemistry,
University of Leoben, Franz-Josef-Str. 18, 8700 Leoben, Austria

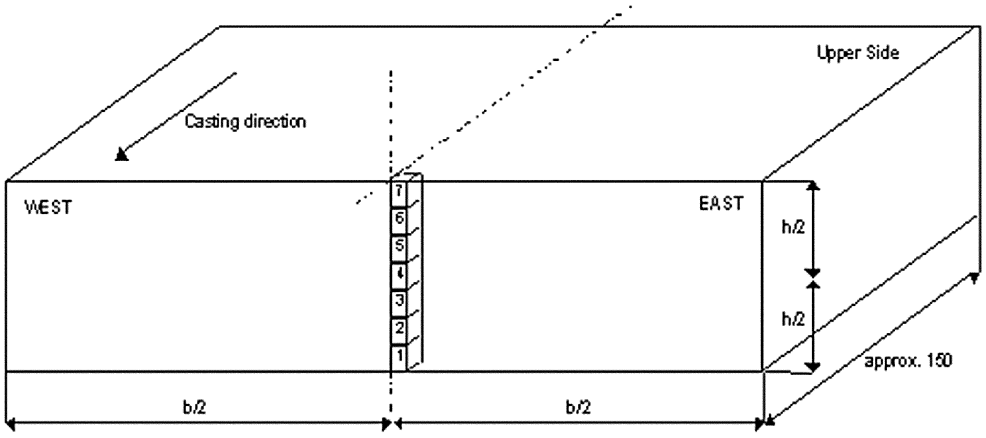

Fig. 2 Position of the slab samples

Table 1 SEM/EDX conditions used for inclusion analysis

Beam energy	15 kV
Emission current	30–35 µA
Vacuum pressure	8×10^{-4} Pa
Working distance	18–20 mm
Detector mode	BSE
Magnification	600×
Detectable inclusion sizes	1–130 µm
EDX-analysis duration for evaluated particles	3 s
Detection limits for 3 s EDX-analysis (element dependent)	0.3–1.1 m-%
Electron raster style during EDX-analysis	Feret raster (Fig. 4)

uation after data acquisition are outlined. The strengths and limitations of the developed procedure are subsequently discussed using low-carbon (LC) steel analysis as an example.

Experimental

Sampling

Cleanliness measurements by automated SEM/EDX analysis are usually done on slab or strip samples. For investigations discussed in this paper seven slab samples taken one above the other (Fig. 2) were analysed.

Sample preparation

For cleanliness investigations at **voest**alpine a metallographic preparation technique has been optimised. First the samples are ground manually with SiC paper (granulation 180 to 1200) and then are polished semi-automatically using ethanol as lubricant. Special polishing cloths, 3 µm and afterwards 1 µm diamond suspension, are used for optimal sample preparation.

It is absolutely essential to check the result of the preparations under an optical microscope. This is necessary to ensure only a few abrasive grains are detectable in the surface and to check that the inclusions have not broken loose during metallographic preparation [4].

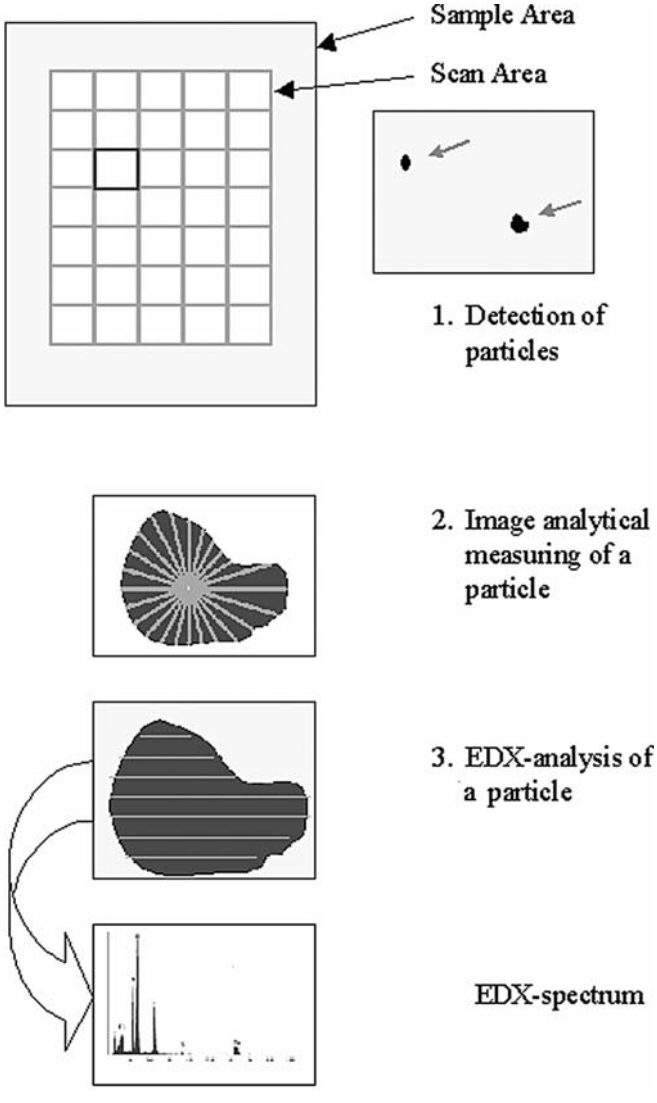

Fig. 3 Principle of the automated search and analysis mechanism of the P-SEM

Specifications of the SEM/EDX system

The basis of inclusion analysis is a conventional scanning electron microscope (SEM) with tungsten filament and secondary electron (SE) and back-scattered electron (BSE) detectors working at vac-

Table 2 Explanation of inclusion classes

Class	Inclusion type	Description
1	Al_2O_3	Alumina inclusion
2	CA	Calcium aluminate
3	CA-CaS	Calcium aluminate with calcium sulfide
4	CA-(Ca, Mn)S	Calcium aluminate with calcium, manganese sulfide
5	$MgO.Al_2O_3$	Magnesium spinel
6	$MnO.Al_2O_3$	Manganese spinel (galaxite)
7	Mn-Silicate	Manganese silicate
8	Al-Silicate	Aluminium silicate
9	Mn-Al-Silicate	Manganese-aluminium silicate
10	CaO-CaS	Calcium oxide or calcium oxide with calcium sulfide
11	(Mn,Fe)S	Manganese-iron sulfide
12	TiS	Titanium sulfide
13	(Mn,Fe,Ti) S	Manganese-iron-titanium sulfide
14	CaS	Calcium sulfide
15	(Mn,Fe,Ca,Ti,Mg) S	Manganese-iron-calcium-titanium-magnesium sulfide
16	OS	Oxisulfide (endogenous oxide with sulfide)
17	OCN	Oxi-carbo-nitride
18	OCN-S	Oxi-carbo-nitride with sulfide
19	CN	Carbo-nitride
20	CN-S	Carbo-nitride with sulfide
21	Exogenous+Na	Exogenous inclusion with sodium content
22	Exogenous	Exogenous inclusion
23	Unid	Particle not categorised

uum pressure. Elemental information of each analysed inclusion is determined by use of a lithium drifted energy-dispersive silicon X-ray detector (EDX). The conditions used for inclusion analysis are shown in Table 1.

Inclusion analysis by automated SEM/EDX-measurement

With the help of a software tool especially developed for particle analysis the sample stage can be driven and the samples are analysed completely automatically by searching a user-specified area for non-metallic inclusions. The contrast in BSE-mode is strongly dependent on the atomic number of the searched point. Points of high atomic number are shown brightly, points of low atomic number are displayed darkly [5, 6]. Non-metallic inclusions usually have much lower atomic numbers than the steel matrix. Dark features are distinguished from the bright steel matrix using a threshold criterion based on pixel intensity [7].

When a particle is detected it is characterized with a rotating chord algorithm (an example is shown in Fig. 3). This algorithm finds the centre of the particle and draws 16 chords through the centre at constant degree intervals.

As a result a set of size and shape data are computed from the lengths of the chords. An energy dispersive X-ray (EDX) spectrum is then taken to obtain the elemental composition of the particle. This is done by scanning the inclusion in the form of lines.

On the basis of the determined elemental composition, features that fail to meet a self-defined rejection criterion are excluded online. Information about all the other particles is stored in a raw data file [8].

Subsequently an offline evaluation programme is applied that makes it possible to classify the detected particles into inclusion classes. Because X-rays are not only emitted by the inclusion itself but also by the surrounding steel matrix the iron content is set to zero and an appropriate content of the other alloying elements in the steel matrix is subtracted. The elemental composition of each particle is then renormalized to a total of 100%. These calculations are necessary for correct classification of inclusions, because the iron content is more strongly influenced by the size than by the iron content of the inclusion itself. The smaller the detected particle the larger is the iron content in the spectrum, because more X-rays are emitted from the steel matrix. From this it follows that the inaccuracy of the results rises if the average diameter of the analysed particles becomes smaller. Based on the assumption that inclusions do not contain iron (which is true for almost every inclusion type) the programme recalculates the composition of all particles. Otherwise alloying elements would be overestimated in the results of EDX quantification.

For classification the renormalized data of the particles is run through an evaluation algorithm which categorises the particles into 23 inclusion classes (Table 2 shows the inclusion classes with their abbreviations).

The evaluation programme also calculates the diameter of a circle with equal area (Dcircle) and the length/width ratio (Dratio) characterizing the size and shape of each particle.

A "Details" table showing the results for each particle can be very helpful in case of doubt. But this table does not give the summarized information about the inclusions necessary for comparison of results from different steel samples. For this reason a summary table and a set of different diagrams are created to give a clearer picture of the inclusion chemistry in the sample.

Results from an LC steel will demonstrate the strengths of this evaluation routine.

Results and discussion

The steel samples investigated

An LC steel slab was sampled as shown in Fig. 2. The composition of the LC melt is shown in Table 3.

Results from offline evaluation of the analysed LC steel

Results from offline evaluation are shown on example of one of the seven LC steel samples analysed. The summary table shown in Fig. 4 contains the most important facts about the analysed micro-inclusions in the sample: dominant inclusion classes, average size, shape and composition of each class. It is composed of a set of independent tables. On the top are smaller tables which give information about the total area scanned, the total number of particles and average particle sizes.

The big table underneath gives summarized information about each of the 23 inclusion classes. The results of

Table 3 Chemical composition of the investigated LC-steel (in m-%)

C	Mn	Al	Si	P	S	N	Nb+Ti+V
0.049	0.21	0.045	0.01	0.01	0.01	0.004	0.005

Scanned Area Total	
Area / mm²	102.7
Content / µm²/mm²	58.2

Total # Particles	
measured	1186
excluded	32
evaluated	1154

Avrg Part. Sizes	
Area / µm²	5.0
Dcircle / µm	2.5

	Results of Image Analysis						Results of EDX-Analysis (without C, N and O)												
	Num	Num	Area	Dcirc	D-ratio	Content	Al	Ca	Mg	Si	S	Mn	Ti	Na	K	Cr	P	Cl	CaO/Al2O3
	ptcls	%	%	µm	µm/µm	µm²/mm²	m-%	m-%	m-%	m-%	m-%	m-%	m-%	m-%	m-%	m-%	m-%	m-%	m-%/m-%
Excl	32																		
A	193	16.7	27.4	3.3	1.6	16.0	92	0	3	0	1	1	0	0	0	0	0	1	
CA	24	2.1	2.8	3.0	1.7	1.7	85	6	3	0	1	1	1	0	0	1	0	1	0.05
CA+CaS	0	0	0	0	0	0	0	0	0	0	0	0	0	0	0	0	0	0	0.00
CA+(Ca,Mn)S	35	3.0	2.3	2.2	1.5	1.3	55	6	2	0	13	21	1	0	0	1	0	1	0.07
MgO.Al2O3	41	3.6	8.5	4.0	2.0	4.9	85	1	9	0	1	1	0	0	0	1	0	1	
MnO.Al2O3	6	0.5	0.5	2.5	2.3	0.3	81	1	3	0	2	9	1	0	0	1	0	1	
Mn-Silicate	1	0.1	0.0	1.6	1.8	0.0	0	5	0	81	0	14	0	0	0	0	0	0	
Al-Silicate	2	0.2	0.4	3.9	1.3	0.2	42	1	2	45	0	0	1	2	7	0	0	1	
(Mn,Al)-Silicate	1	0.1	0.1	2.0	1.3	0.0	24	0	5	43	0	14	0	0	14	0	0	0	
CaO-CaS	7	0.6	1.1	3.5	1.4	0.7	1	87	2	3	0	0	0	1	1	1	0	2	
(Mn,Fe)S	251	21.8	6.5	1.4	1.7	3.8	1	1	1	0	38	57	0	0	0	1	0	1	
TiS	0	0	0	0	0	0	0	0	0	0	0	0	0	0	0	0	0	0	
(Mn,Fe,Ti)S	0	0	0	0	0	0	0	0	0	0	0	0	0	0	0	0	0	0	
CaS	1	0.1	0.2	3.5	1.9	0.1	0	47	0	0	37	3	0	0	3	3	0	7	
(Mn,Fe,Ca,Ti,Mg)S	17	1.5	1.1	2.2	1.7	0.6	2	1	6	0	45	43	0	0	0	1	0	1	
OS	569	49.3	47.8	2.5	1.6	27.8	54	2	3	0	18	20	0	0	0	1	0	1	
CN	0	0	0	0	0	0	0	0	0	0	0	0	0	0	0	0	0	0	
CNS	0	0	0	0	0	0	0	0	0	0	0	0	0	0	0	0	0	0	
OCN	0	0	0	0	0	0	0	0	0	0	0	0	0	0	0	0	0	0	
OCNS	0	0	0	0	0	0	0	0	0	0	0	0	0	0	0	0	0	0	
Exogenous+Na	0	0	0	0	0	0	0	0	0	0	0	0	0	0	0	0	0	0	
Exogenous	3	0.3	0.5	3.6	1.4	0.3	5	61	5	17	1	2	4	1	2	0	0	3	
Unid	3	0.3	0.9	4.8	1.3	0.5	9	49	1	28	1	1	0	6	1	1	0	2	
Σ	1154	100.0	100.0			58.2													

Fig. 4 Summary table

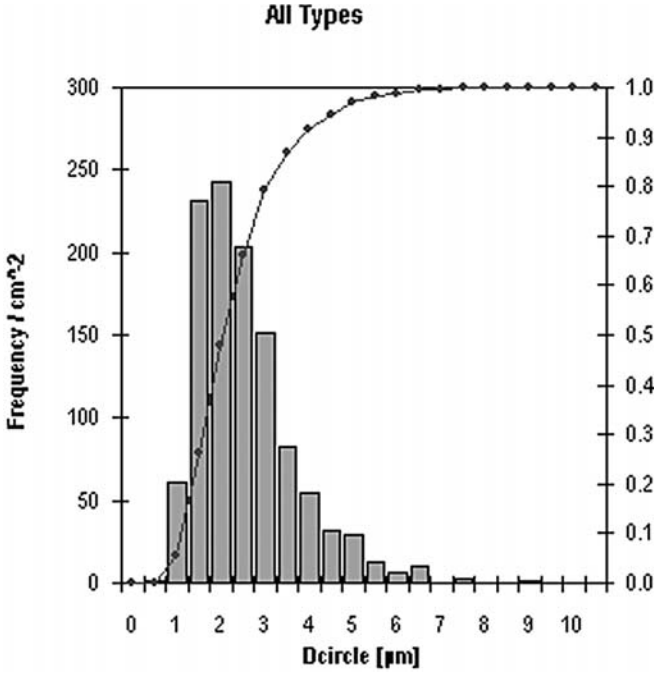

Fig. 5 Size distribution of all inclusions in an LC steel sample

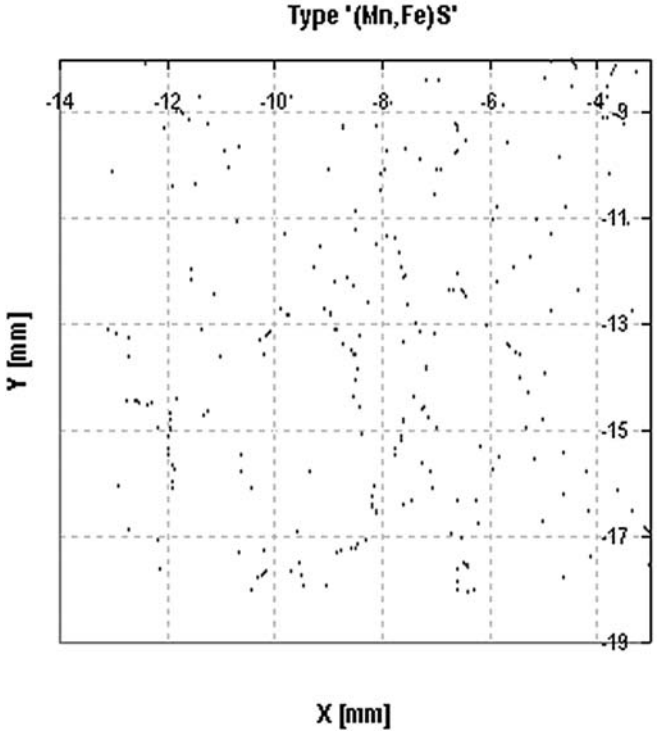

Fig. 6 *XY* distribution of (Mn,Fe)S in the LC steel indicates the primary solidification structure

image analysis (number, number percent, area percent, Dcircle, Dratio, area fraction (in $\mu m^2\,mm^{-2}$)) and the average elemental composition normalized to a total of 100% for the inclusions in each class determined by EDX analysis are shown. At the far right the average CaO/Al_2O_3-ratio is calculated for the calcium aluminate inclusion

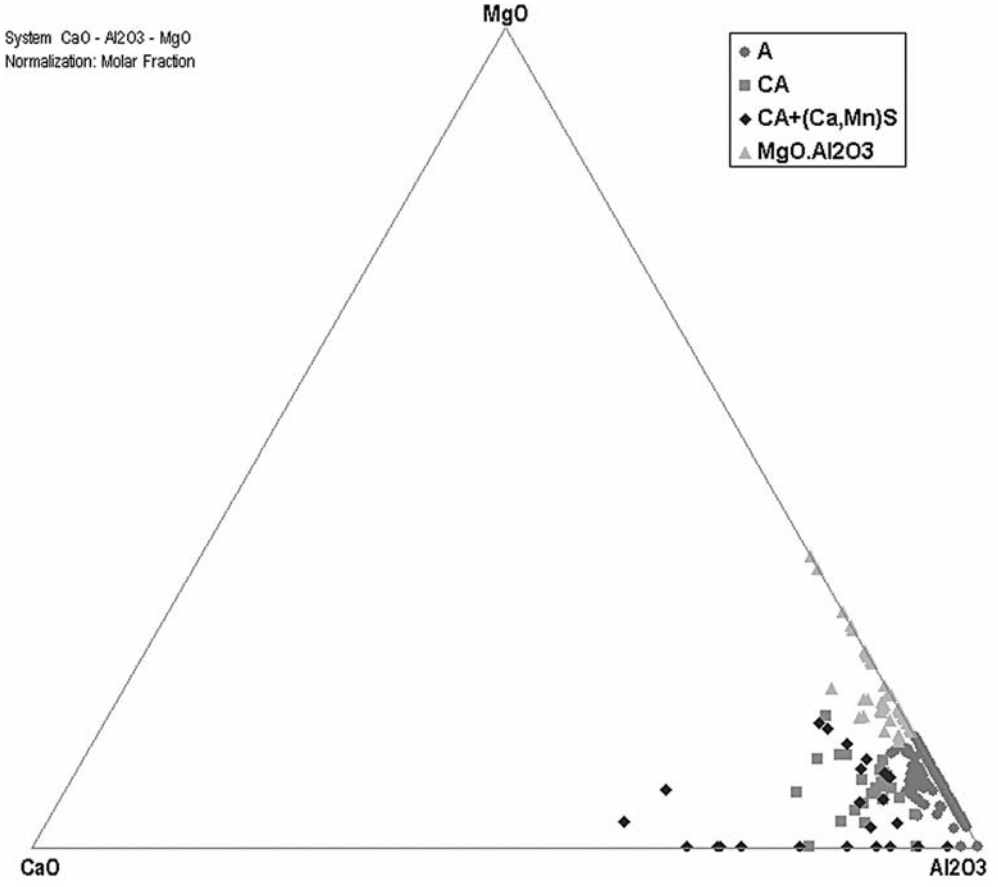

Fig. 7 Ternary diagram MgO–CaO–Al_2O_3

classes to see the phase region of the binary CaO-Al_2O_3 diagram the inclusions can be expected.

The dominant classes (in number-% and area-%) and average sizes (in µm) can also be displayed in bar diagrams. The most important classes in LC steel are the aluminates, MgO.Al_2O_3 spinels, (Mn,Fe)S and oxisulfides; the area content is largest for the latter.

The histogram in Fig. 5 shows the size distribution of all inclusions. Similar diagrams can be produced for each separate inclusion class containing more than 30 inclusions. Inclusion maps are created for all inclusions and for separate inclusion classes to depict the lateral inclusion distribution. Very interesting is the diagram for (Mn,Fe)S precipitation (Fig. 6) which can give a picture of the solidification structure of the steel.

Binary and ternary diagrams are drawn to visualize the composition of the inclusions. The elements in these diagrams can be changed depending on the steel production route and the inclusion types. By stoichiometric calculation of the oxides based on the elemental determination of the inclusions each inclusion is drawn as one point. To distinguish between inclusions of different classes the particles of each class are drawn in a specific colour. The area of high accumulation of points shows the most likely composition of the inclusions. As an example a ternary phase diagram (MgO-CaO-Al_2O_3) for oxide inclusions is shown in Fig. 7.

Fig. 7 confirms that almost all oxides are alumina inclusions in this LC steel. This is the result of aluminium deoxidation and no calcium treatment for inclusion formation during secondary metallurgy.

Final result for the analysed LC slab

Based on seven single results the mean values and the confidence intervals for all inclusion types are calculated (Fig. 8). As expected the dominant inclusion types are the same for

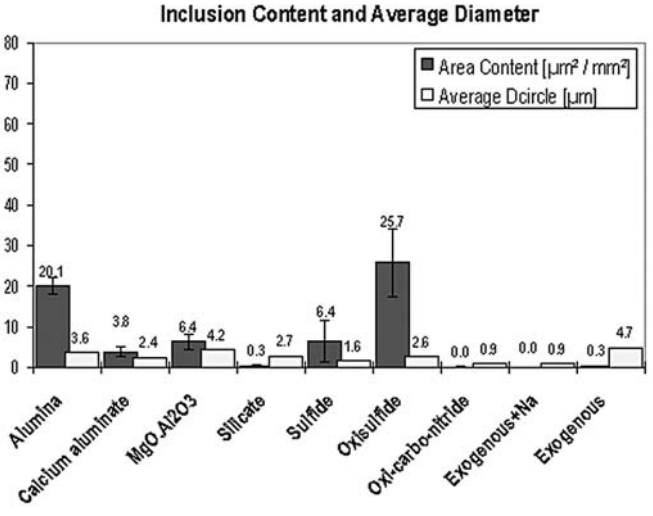

Fig. 8 Final results from seven samples from one LC slab

all seven samples. These are alumina, $MgO.Al_2O_3$ spinel, sulfide and oxisulfide inclusions. The amount of the oxide inclusions is similar in all measurements. Sulfide and oxisulfide inclusion content vary widely. Sample Nr. 4 taken from the middle of the slab has the highest sulfide content with more than $20\,\mu m^2\,mm^{-2}$. This can be easily explained by the effect of macro-segregation of sulfur. On the other hand the strong variation of the oxisulfides can be explained by the effect of micro-segregation of sulfur [9]. Slightly surprising is the appearance of calcium aluminates because no calcium was added during secondary metallurgy. Closer inspection reveals the small amounts of calcium in the calcium aluminate inclusions; these lead to an average CaO/Al_2O_3 ratio of 0.07. This calcium content can enter the steel melt in slag which contains CaO or by calcium contamination of slag forming additions.

Other types of inclusion were also detected but those were just found accidentally. This can be confirmed by the sum of the area contents of alumina and oxisulfide inclusions which make almost 7% of the entire inclusion areas in LC steel.

Conclusion

Inclusion investigations by automated SEM/EDX analysis and evaluation of inclusion contents, size and shape data have been carried out for more than 15 years [7]. Recalculation of the iron and alloying element content have not been mentioned in former publications, but are implemented in the offline evaluation software described in this paper. Elemental composition is determined more exactly and overestimation of alloying elements is also avoided.

Because of these advances the analytical technique presented is suitable for description of the chemical nature of the inclusions. Dominant chemical compounds can be pointed out and provide useful information about the metallurgical production process.

Differences in chemical composition, ladle treatment, casting conditions and differences in samples taken at different manufacturing levels can be shown statistically by this method.

These analyses reveal which amounts of each type of inclusion must be expected in LC steels. In a similar way all steel grades can be investigated. Statistical evaluation of the data with confidence intervals is necessary to obtain correct results the distribution of the inclusions in the steel matrix. This statistical evaluation enables determination of the confidence range in which inclusions of a defined chemical composition appear.

Based on measurements by automated SEM/EDX analysis a complete inclusion catalogue for all different steel grades produced at **voest**alpine-Stahl is generated. With the help of this catalogue changes in metallurgical treatment ought to be pinpointed. This method should therefore lead to an improvement of the cleanliness of conventional steel and also new steel grades.

Acknowledgements The authors gratefully acknowledge financial support of the KnetMET: Industrial Competence network for metallurgical and environmental-technically process development supported by the Federal Ministry for economic affairs and labour, the State of Upper Austria, the State of Styria, and the Steirischen Wirtschaftsförderungsgesellschaft m.b.H.

References

1. Dekkers R (2002) Non-metallic inclusions in liquid steel, Dissertation, University of Leuven
2. Koch E et al (1998) BHM, 143Jg, Heft 9, 338–344
3. Loh J et al (2002) Proc 6th Int Conf On Clean Steel, pp 348–353
4. Angeli J, Flößholzer H, Jandl K, Kaltenbrunner T, Posch W, Preßlinger H (1999) La Revue de Métallurgie-CIT, pp 521–527
5. Jaeger W, Steinberg W, Holtz B, Friedel F (2002) Proc 6th Int Conf On Clean Steel, pp 280–285
6. Flegler S, Heckman J, Klomparens K (1995) Elektronenmikroskopie. Spektrum Akademischer, Heidelberg
7. Kluken O et al (1988) Mater Sci Technol 4:649–654
8. Ritchie N (2001) Aspex, LLC, Delmont, USA, Automated Feature Analysis for Perception, User's Documentation
9. Schwerdtfeger K (1991) Metallurgie des Stranggießens. Stahleisen, Düsseldorf